

Fuzzy Based Traversability Analysis for a Mobile Robot on Rough Terrain

Yusuke Tanaka¹, Yonghoon Ji¹, Atsushi Yamashita¹, and Hajime Asama¹

Abstract—We present a novel rough terrain traversability analysis method for mobile robot navigation. We focused on the scenario of mobile robot operation in a disaster environment with limited sensor data. The robot builds a map in real time and analyzes the terrain traversability of its surrounding environment. The proposed method is based on fuzzy inference so that it can handle uncertainties in the sensor data. Two values associated with the terrain traversability, roughness and slope, are calculated from an elevation map built by a laser range finder mounted on the mobile robot. These two values are inputted to the fuzzy inference, and the traversability is analyzed. Based on the traversability output from the fuzzy inference, a vector field histogram (VFH) is generated. The mobile robot course is determined according to the VFH. We demonstrated our algorithm on an artificial environment. The experimental results showed that the mobile robot was able to reach the target position safely while avoiding untraversable areas.

I. INTRODUCTION

Robots have attracted the attention of a large number of researchers and are becoming capable of dealing with complex environments [1]. Innovations involving the application of mobile robots to investigating disaster sites and assisting with agriculture have increased [2]. In these situations, the navigation and obstacle avoidance of mobile robots is a major challenge. In the last few years, some breakthroughs have been made to solve these problems. The Defense Advanced Research Projects Agency (DARPA) Grand Challenge showed that unmanned ground vehicles (UGVs) can navigate a highly controlled desert area [3]-[5]. In this challenge, one of the main problems was mobile robot navigation on rough terrain. For most mobile robot operations in an outdoor environment, rough terrain is a problem. Terrain negotiation becomes a particular problem when operating robots at disaster sites. One of the main reasons for the difficulty is the uncertainty over the terrain state caused by limited sensor data. In a messy environment, sensors commonly go out of order, and acquired information becomes uncertain or noisy. Because of the limited sensor configuration, perfect understanding of the surrounding environment may be impossible. In order to complete investigations or rescue tasks, the operator or robot itself has to compensate for the limited sensor data and proceed over unstructured inaccessible areas [6].

With regard to traversal over rough terrain, selecting the appropriate course and direction of the mobile robot is vital. The mobile robot has to avoid untraversable areas and select

only traversable areas while making its way to the target position. In order to appropriately judge the course direction, terrain traversability analysis (TTA) is important. In short, accurately representing the terrain state and analyzing it in real time is a challenge for most mobile robots.

II. RELATED RESEARCH

Because of the importance of robotic vehicle mobility, many studies have examined obstacle avoidance and TTA for mobile robots. Borenstein et al. proposed the vector field histogram (VFH) method along with improved versions, where the risk around the mobile robot is expressed in the form of a histogram, and the robot selects a safe course and direction [7]-[9]. In this method, the distance between the mobile robot and obstacles is measured by an ultrasonic sensor or laser range finder (LRF) mounted on the mobile robot. A binary expression grid-type map of the environment is built based on the measured distances. The VFH generates risk values for the environment that are converted from the distance information. The VFH is less likely to get trapped in local minima and allows mobile robots to move stably [10]. However, this method is limited because of the environment is expressed in binary form. Therefore, the traversability state of the terrain cannot be considered. In order to overcome this shortcoming, Ye et al. proposed the TTA method, which is based on an elevation map and its transformation into a traversability map [11]-[13]. In this method, an elevation map of the environment is built from laser range finder measurements. The elevation map is called a “2.5-D map” and represents the height information in grid-type cells. The constructed elevation map is then transformed into a traversability map where the traversability value is expressed in the form of grid-type cells. In this method, a relatively large amount of height information is needed to provide reasonable performance [14].

Some researchers have employed the terrain classification approach based on principal component analysis [15], [16]. In these methods, point cloud data of the environment are gathered and grouped for classification into eigenvectors. The eigenvector’s magnitude and orientation give the point cloud’s shape, inclination and unevenness. From this information, the traversability of the surrounding environment can be analyzed. This method is limited because it depends on the amount of point cloud data. The classification results become less reliable with less acquired point cloud data. For successful classification and traversability analysis, a relatively large amount of point cloud information is necessary.

¹Y. Tanaka, Y. Ji, A. Yamashita, and H. Asama are with the School of Engineering, The University of Tokyo, 113-8656 Tokyo, Japan (tanaka, ji, yamashita, asama)@robot.t.u-tokyo.ac.jp

The above methods lack viability with regard to their application in messy environments such as disaster sites. In such an environment, the sensing range is limited, and the sensor measurement data are not precise. In order to deal with the TTA problem using limited sensor data, new kind of approach is necessary.

In this paper, we propose a novel TTA method for mobile robot navigation that can work effectively with limited sensor data. To overcome the limited sensor data problem, we adopt fuzzy inference-based TTA. Fuzzy inference allows for reliable traversability analysis from limited sensor data [17]-[20]. With fuzzy inference, we can overcome the previous method's shortcomings and apply our method to disaster environments where sensor measurement data are limited. Our method uses fuzzy inference-based TTA to express the risk around the mobile robot in the form of a VFH. The paper is organized as follows. Section III gives a brief overview of the proposed method. Section IV explains the terrain-related value calculations. Section V presents the proposed fuzzy inference-based TTA. In Section VI, we describe the VFH generation procedure and robot course and direction judgment in detail. In Section VII, we present the experimental validation of the proposed algorithm using a physical robot. Section VIII presents the overall conclusions.

III. OVERVIEW OF PROPOSED METHOD

Figure 1 shows a system overview of our TTA method. Our method can be divided into five main modules: elevation map construction, roughness and slope calculation, fuzzy inference, VFH generation, and direction judgment. In this section, we present a brief explanation of the overall system.

The elevation map construction module builds an elevation map from point cloud data which is acquired by a LRF. For elevation map construction, only the height information of the area surrounding the robot center point (RCP) is needed.

The roughness and slope calculation module calculates these two values around the RCP. First, the elevation map data are divided into rectangular areas. These rectangular areas radiate from the RCP. The roughness and slope are calculated for each rectangular area.

The fuzzy inference module integrates the two values calculated in the previous module to output the traversability value. The module has two membership functions, fuzzy rule, and defuzzifier. These are all original designs for TTA.

The VFH generation module associates the traversability value with the course direction of the mobile robot. During this process, the traversability value is transformed into a risk value for the environment surrounding the RCP.

The direction judgment module selects the course direction of the mobile robot based on the generated VFH information. The method described in the following sections was tested with datasets gathered from an artificial environment. A real robot and related instruments were used in the experiment.

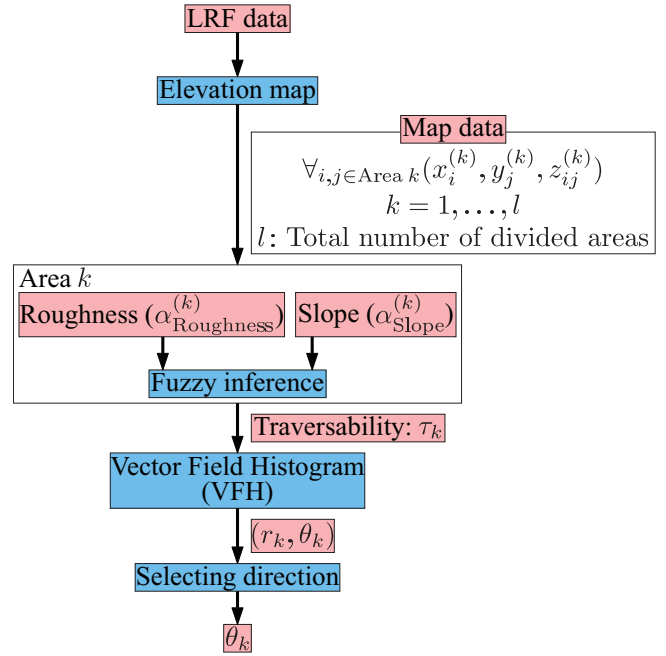


Fig. 1. System overview of proposed method.

IV. CALCULATION OF ROUGH TERRAIN RELATED VALUES

A. Elevation map construction

The elevation map is constructed from range data acquired by a LRF. All elements of the elevation map consist of x , y , and z coordinates. Each position in the environment can be expressed as (x_i, y_j, z_{ij}) . x_i and y_j correspond to cell (i, j) . z_{ij} can be a real value that expresses the height of point (x_i, y_j) . During map construction, the elevation value of each cell is updated as follows:

$$e_{ij}^{(t)} = \begin{cases} z_{ij}^{(t)} & (e_{ij}^{(t-1)} < z_{ij}^{(t)}) \\ e_{ij}^{(t-1)} & (\text{otherwise}) \end{cases}, \quad (1)$$

Here, $e_{ij}^{(t)}$ is the elevation value of cell (x_i, y_j) at time t , $z_{ij}^{(t)}$ is the sensed elevation of cell (x_i, y_j) at time t . This formulation means that if the newly-sensed elevation value at cell (x_i, y_j) is higher than the previous one, then the elevation value at cell (x_i, y_j) is replaced by this new elevation value. Ye and Boresnstein [21], Lee and Ji [22] give the details on construction based on range data.

B. Division of elevation map into rectangular areas

After the elevation map is constructed, the mobile robot anterior region is divided into rectangular areas. These rectangular areas radiate from the RCP. Figure 2 shows the elevation map division. Some parameters are set for dividing the rectangular areas to align the traversability calculation with the characteristics of the environment and robot. Two values related to rough terrain, roughness $\alpha_{\text{Roughness}}^{(k)}$ and slope $\alpha_{\text{Slope}}^{(k)}$, are calculated for each rectangular area. In Figure 2, L is the length of each rectangular area, W is the

width, and θ_k is the angle of the rectangular area's direction vector from the x coordinate of the mobile robot.

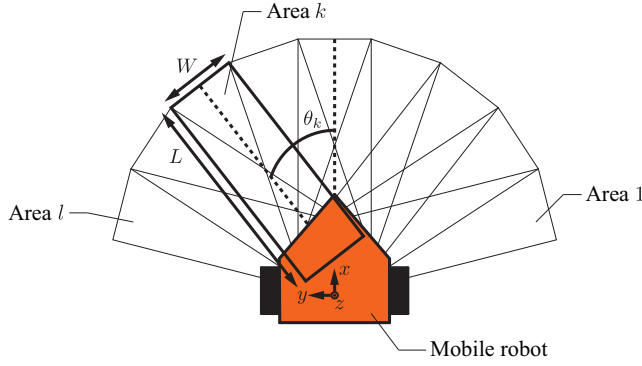


Fig. 2. Elevation map division into rectangular areas.

C. Roughness calculation

Roughness is defined as the standard deviation of the height in each rectangular area. Each rectangular area is expressed with the index k . The roughness $\alpha_{\text{Roughness}}^{(k)}$ is calculated as follows:

$$\alpha_{\text{Roughness}}^{(k)} = \sqrt{\frac{1}{N_k} \sum_{i,j \in \text{Area } k} (z_{ij}^{(k)} - \bar{z}_k)^2}, \quad (2)$$

where

$$\bar{z}_k = \frac{1}{N_k} \sum_{i,j \in \text{Area } k} z_{ij}^{(k)},$$

Here, N_k is the number of cells in each rectangular area, $z_{ij}^{(k)}$ is the height information of cell (i, j) in the rectangular area k , and \bar{z}_k is the average height in each rectangular area.

D. Slope calculation

The slope value of the rectangular area k is calculated from the normal vector of the fitted plane and the direction vector of the rectangular area. The plane fitting is calculated by using all of the height information for the rectangular area k .

The fitted plane in each rectangular area is expressed in the form of the following function:

$$z^{(k)} = a_k x^{(k)} + b_k y^{(k)} + c_k, \quad (3)$$

Here, $\mathbf{n}_k = (-a_k, -b_k, 1)$ is the normal vector of the fitted plane, and $x^{(k)}, y^{(k)}, z^{(k)}$ are the variances which are defined on the rectangular area k . The plane fitting process involves the following optimization:

$$f_k = \sum_{i,j \in \text{Area } k} (a_k x_i^{(k)} + b_k y_j^{(k)} + c_k - z_{ij}^{(k)})^2, \quad (4)$$

$$(a_k, b_k, c_k) = \underset{(a_k, b_k, c_k)}{\operatorname{argmin}} f_k, \quad (5)$$

Here, $x_i^{(k)}, y_j^{(k)}, z_{ij}^{(k)}$ are the values of each cell. This optimization problem can be solved by the following calculation:

$$\begin{pmatrix} a_k \\ b_k \\ c_k \end{pmatrix} = \mathbf{P}^{-1} \mathbf{Q}, \quad (6)$$

where

$$\mathbf{P} = \begin{pmatrix} \sum_{i,j} (x_i^{(k)})^2 & \sum_{i,j} x_i^{(k)} y_j^{(k)} & \sum_{i,j} x_i^{(k)} \\ \sum_{i,j} x_i^{(k)} y_j^{(k)} & \sum_{i,j} (y_j^{(k)})^2 & \sum_{i,j} y_j^{(k)} \\ \sum_{i,j} x_i^{(k)} & \sum_{i,j} y_j^{(k)} & N_k \end{pmatrix},$$

$$\mathbf{Q} = \begin{pmatrix} \sum_{i,j} x_i^{(k)} z_{ij}^{(k)} \\ \sum_{i,j} y_j^{(k)} z_{ij}^{(k)} \\ \sum_{i,j} z_{ij}^{(k)} \end{pmatrix},$$

Through these calculations, the normal vector of the fitted plane $\mathbf{n}_k = (-a_k, -b_k, 1)$ can be acquired. The inner product of this normal vector \mathbf{n}_k and the direction vector \mathbf{d}_k of the rectangular area k generates the slope value $\alpha_{\text{Slope}}^{(k)}$:

$$\alpha_{\text{Slope}}^{(k)} = \left| \cos^{-1} \left(\frac{\mathbf{n}_k \cdot \mathbf{d}_k}{|\mathbf{n}_k|} \right) - \frac{\pi}{2} \right|, \quad (7)$$

where

$$\mathbf{d}_k = \begin{pmatrix} \cos \theta_k \\ \sin \theta_k \\ 0 \end{pmatrix}.$$

V. FUZZY INFERENCE FOR TRAVERSABILITY ESTIMATION

A. Fuzzy inference model

In our method, the terrain traversability is estimated with a fuzzy inference framework. The roughness and slope from the previous module are inputted to output the traversability value of each rectangular area. We adopted the Mamdani fuzzy model, which is a typical fuzzy inference model, for our method [23].

B. Membership functions

We developed two original membership functions, one for the roughness and the other for the slope, and tuned them for traversability estimation. Figure 3 shows the two membership functions.

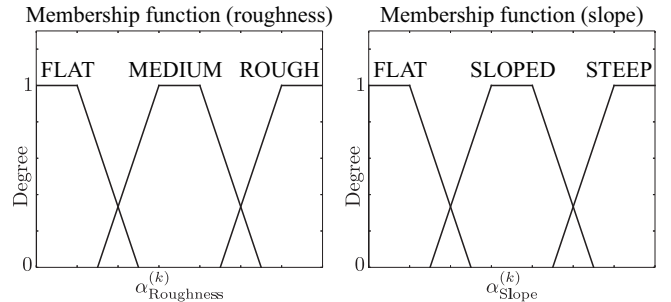


Fig. 3. Two membership functions.

Each membership function outputs the degree-of-membership of the rectangular area for one real value input. The extent of the roughness {FLAT, MEDIUM, ROUGH} is estimated with the membership function. The extent of the slope {FLAT, SLOPED, STEEP} is also estimated with

the membership function. We adopted trapezoid-shaped functions for our method. Therefore, each membership function has two intersection points for one input value. The degree-of-membership and extent label are assigned to each intersection point. Each membership function eventually outputs two degree-of-membership and extent label pairs.

C. Fuzzy rule

The fuzzy rule determines the degree of membership and the extent label for the traversability. In the Mamdani fuzzy model, the fuzzy inference process can be divided into two parts: label integration and logical product. Figure 4 shows the fuzzy rule matrix. In the label integration part, the traversability extent label is judged based on the rule matrix. The inputs of the rule matrix are the roughness and slope labels, and the output is the traversability label. The traversability extent label is taken from the set {HIGH, MODERATE, LOW, POOR}. In the logical product part, the roughness and slope degrees of membership are compared, and the smaller is adopted as the input of the defuzzifier.

		Roughness		
		FLAT	MEDIUM	ROUGH
Slope	FLAT	HIGH	MODERATE	POOR
	SLOPED	MODERATE	LOW	POOR
	STEEP	POOR	POOR	POOR

Fig. 4. Fuzzy rule matrix.

D. Defuzzifier

The defuzzifier outputs the traversability value τ_k as the centroid of all input information pairs. Figure 5 shows the defuzzifier. Each degree-of-membership and extent label pair for the traversability is reflected by the trapezoids for the defuzzifier. The centroid is calculated from these trapezoids. The output traversability value τ_k is acquired from the centroid point about the horizontal axis of the defuzzifier.

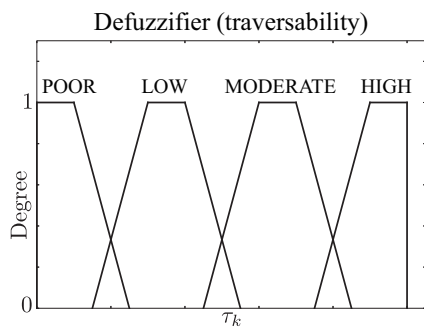


Fig. 5. Defuzzifier.

VI. COURSE DIRECTION JUDGEMENT FROM VECTOR FIELD HISTOGRAM

A. Vector Field Histogram (VFH)

The VFH shows the risk value of the environment. In our method, each rectangular area's risk value is transformed from the traversability value as follows:

$$r_k = \frac{1}{\tau_k}, \quad (8)$$

These risk values are expressed on the vertical axis of the VFH, and the horizontal axis represents the rectangular area's direction. Figure 6 shows an example of a generated VFH. A rectangular area with a low risk value means that the area can be traversed by a mobile robot. On the other hand, a high risk value means that the area is hard to traverse.

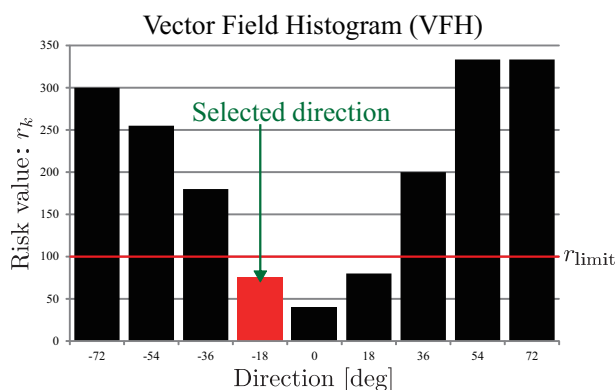


Fig. 6. VFH example.

B. Course direction judgment

The mobile robot judges the course direction based on the risk value threshold and distance between the target position and rectangular area. First, the robot searches for rectangular areas with risk values under the threshold. The rectangular area under this threshold and with the shortest distance to the target position is then selected as the course direction of the mobile robot.

VII. EXPERIMENTAL RESULTS

To test our TTA method, we constructed the artificial environment shown in Figure 7b. We used a Pioneer 3DX mobile robot with a HOKUYO UTM-30LX laser range finder mounted on top of the robot. These instruments are shown in Figure 7a. One of our main objectives with this new method was to provide a system that can analyze the traversability of rough terrain and make decisions about which direction the mobile robot should go. In our experiment, all of our results were based on real data collected from the laser range finder. At critical instances that required correct traversability analysis and course direction judgment, we confirmed that the proposed method successfully selected a traversable direction as the mobile robot's course. On the other hand, we implemented and tested another method explained in [11] as the conventional method. During experimental operation, we

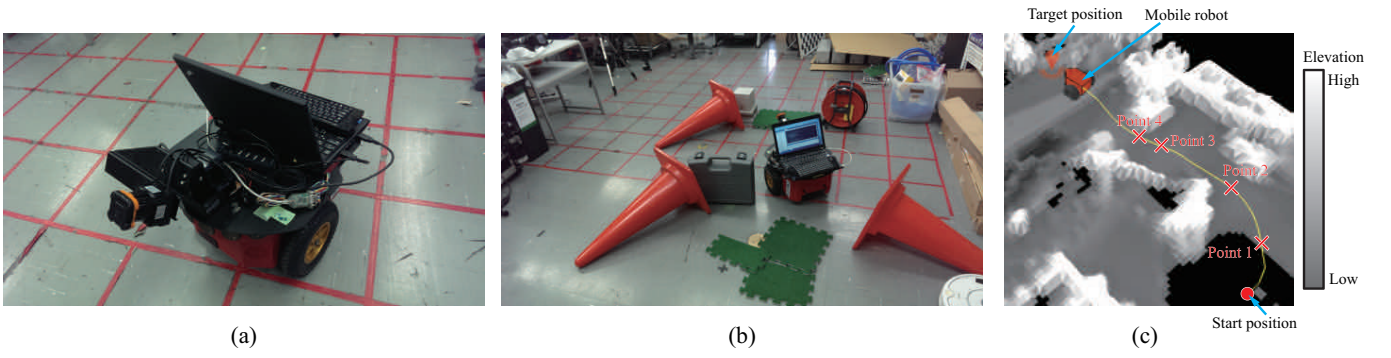


Fig. 7. Experimental pictures: (a) a Pioneer 3DX mobile robot with a laser range finder, (b) constructed artificial environment, and (c) generated elevation map and mobile robot's path during experimental operation.

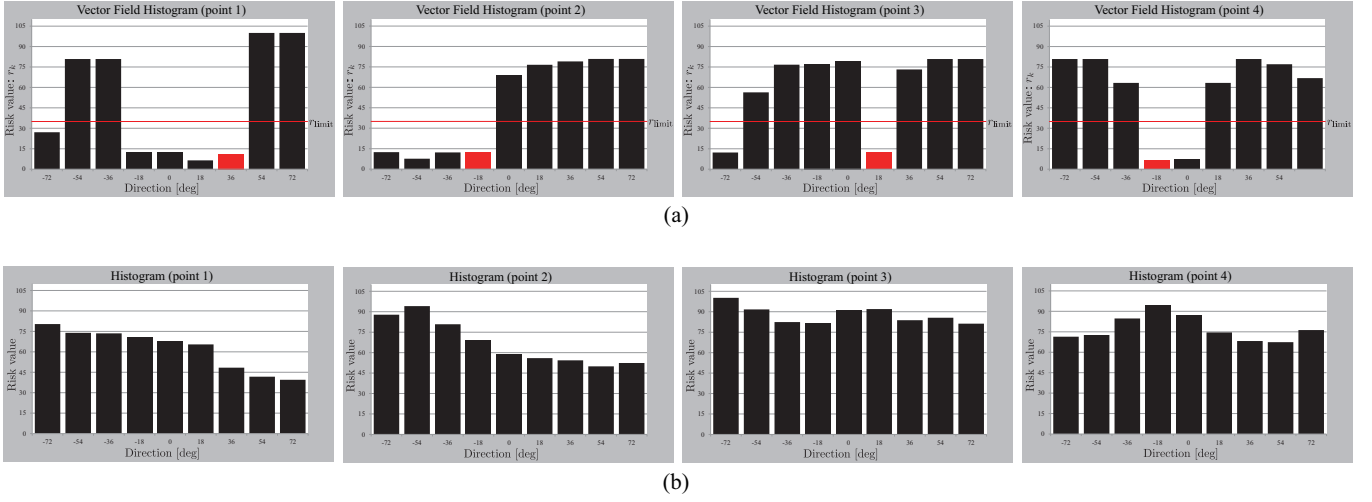


Fig. 8. Comparison of generated VFHs during experimental operation: (a) VFHs generated by proposed method and (b) VFHs generated by conventional method.

gathered two results from different methods and compared them.

In our experiment, the values of each parameter were as follows: $L = 1.0$ m, $W = 0.5$ m, number of all rectangular areas $l = 9$, risk value threshold $r_{\text{limit}} = 35$. The elevation map cell size was 50×50 mm. For the conventional method's parameter, we set 2.0×2.0 m square area patch size. Histograms were generated from height information in this patch. It should be noted that description in [11] said appropriate patch size was 9.2×9.2 m.

In this section, we present the experimental results. Figure 7c shows the mobile robot's path over the constructed rough terrain. The run started at the start point and terminated at the target position. Our entire algorithm was performed in real-time. The yellow line shows the robot's path as estimated by odometry.

Figure 8 compares the VFHs generated during the experiment. We compared two VFHs: one from our proposed method and the other from the conventional method. As noted before, our proposed method generated clear VFHs, and the appropriate course direction for the mobile robot was selected despite the limited sensor data acquisition area. The limited sensor data acquisition area meant that our method

only needs the height information of the rectangular areas to generate a VFH. On the other hand, Figure 8b (point 1)-Figure 8b (point 4) show that the conventional method could not produce a reasonable performance in terms of VFH generation with limited height information. The height information in these figures was over almost the same area size as that used for our proposed method.

The robot first steered and reached point 1. The VFH at this point is Figure 8a (point 1). Since most of the rectangular areas included relatively flat area, their risk values were relatively low and some of them had risk values under threshold r_{limit} . Among them, one which had the shortest distance between the preset target position and the rectangular area was chosen as a course direction. The robot then moved to point 2. At this point, the VFH is depicted in Figure 8a (point 2). At point 2, relatively steep height variances and inclinations were came into some rectangular areas because of the existence of obstacles. In this situation, the robot could choose traversable path between these obstacles. According to VFH information, the robot correctly selected the passage between obstacles (from point 2 to point 3). After point 3, the robot steered to the passage between obstacles again. Figure 8a (point 4) shows that the course direction

judgment at point 4 was over the direction of the traversable rough terrain area.

VIII. CONCLUSIONS

In conclusion, we developed a novel terrain traversability analysis method for mobile robot navigation. In the proposed method, we introduce a new framework for TTA and VFH generation. This approach allows TTA and judging a mobile robot's course direction when sensor information is limited and a large area map of the environment is not available.

Our algorithm first extracts the roughness and slope from an elevation map created from point cloud measurement data. These two values are inputted to the fuzzy inference module, and the traversability is calculated based on the fuzzy rule and defuzzifier. This traversability value is transformed into a risk value. The risk value is expressed in the form of a VFH, which is a method developed for obstacle avoidance. The mobile robot's course direction is selected from the VFH.

The experimental results showed that our algorithm reliably allows the mobile robot to navigate to the target position while avoiding untraversable areas. During the experiment, the robot selected traversable areas of the rough terrain to make its way to the target position. The comparison of our proposed method and the conventional method showed the reliability of our method in spite of the limited sensor data acquisition area. Currently, validation of the system is ongoing with further experiments being performed with real robots.

ACKNOWLEDGMENT

This work was in part supported by Tough Robotics Challenge, ImpACT Program (Impulsing Paradigm Change through Disruptive Technologies Program).

REFERENCES

- [1] C. H. Chen, Y. Weng, and C. T. Sun: "Toward the Human-Robot Co-Existence Society: On Safety Intelligence for Next Generation Robots," *International Journal of Social Robotics*, vol. 1, no. 4, pp. 267–282, 2009.
- [2] S. Tadokoro: "Special Project on Development of Advanced Robots for Disaster Response (DDT Project)," *Proceedings of the 2005 IEEE Workshop on Advanced Robotics and its Social Impacts*, pp. 66–72, 2005.
- [3] C. Crane, D. Armstrong, R. Touchton, T. Galluzzo, S. Solanki, J. Lee, D. Kent, M. Ahmed, R. Montane, S. Ridgeway, S. Velat, G. Garcia, M. Griffiths, S. Gray, J. Washburn, and G. Routson: "Team CIMAR's NaviGATOR: An Unmanned Ground Vehicle for the 2005 DARPA Grand Challenge," *Journal of Field Robotics*, vol. 23, no. 8, pp. 599–623, 2006.
- [4] S. Thrun, M. Montemerlo, H. Dahlkamp, D. Stavens, A. Aron, J. Diebel, P. Fong, J. Gale, M. Halpenny, G. Hoffmann, K. Lau, C. Oakley, M. Palatucci, V. Pratt, P. Stang, S. Strohband, C. Dupont, L. E. Jendrossek, C. Koelen, C. Markey, C. Rummel, J. V. Niekerk, E. Jensen, P. Alessandrini, G. Bradski, B. Davies, S. Ettinger, A. Kaehler, A. Nefian, and P. Mahoney: "The Robot That Won the DARPA Grand Challenge," *Journal of Field Robotics*, vol. 23, no. 9, pp. 661–692, 2006.
- [5] S. Thrun, M. Montemerlo, and A. Aron: "Probabilistic Terrain Analysis For High-Speed Desert Driving," *Proceedings of Robotics: Science and Systems*, pp. 16–19, 2006.
- [6] C. J. M. Kruijff, V. Tretyakov, T. Linder, F. Pirri, M. Gianni, P. Papadakis, M. Pizzoli, A. Sinha, E. Pianese, S. Corrao, F. Priori, S. Febrini, and S. Angeletti: "Rescue Robots at Earthquake-Hit Mirandola, Italy: A Field Report," *Proceedings of the 2012 IEEE International Symposium on Safety, Security, and Rescue Robotics*, pp. 1–8, 2012.
- [7] J. Borenstein and Y. Koren: "The Vector Field Histogram-Fast Obstacle Avoidance for Mobile Robots," *IEEE Transactions on Robotics and Automation*, vol. 7, no. 3, pp. 278–288, 1991.
- [8] I. Ulrich and J. Borenstein: "VFH+: Reliable Obstacle Avoidance for Fast Mobile Robots," *Proceedings of the 1998 IEEE International Conference on Robotics and Automation*, pp. 1572–1577, 1998.
- [9] I. Ulrich and J. Borenstein: "VFH*: Local Obstacle Avoidance with Look-Ahead Verification," *Proceedings of the 2000 IEEE International Conference on Robotics and Automation*, pp. 2505–2511, 2000.
- [10] A. Manz, R. Liscano, and D. Green: "A Comparison of Realtime Obstacle Avoidance Methods for Mobile Robots," *Experimental Robotics*, 1991.
- [11] C. Ye and J. Borenstein: "A Method for Mobile Robot Navigation on Rough Terrain," *Proceedings of the 2004 IEEE International Conference on Robotics and Automation*, pp. 3863–3869, 2004.
- [12] C. Ye and J. Borenstein: "T-transformation: Traversability Analysis for Navigation on Rugged Terrain," *Proceedings of the Defense and Security Symposium, Unmanned Ground Vehicle Technology VI (OR54)*, pp. 12–16, 2004.
- [13] C. Ye: "Navigating a Mobile Robot by a Traversability Field Histogram," *IEEE Transactions on Systems, Man, and Cybernetics, Part B: Cybernetics*, vol. 37, no. 2, pp. 361–372, 2007.
- [14] S. Choi, E. Kim, and S. Oh: "Real-Time Navigation in Crowded Dynamic Environments Using Gaussian Process Motion Control," *Proceedings of the 2014 IEEE International Conference on Robotics and Automation*, pp. 3221–3226, 2014.
- [15] J. F. Lalonde, N. Vandapel, D. F. Huber, and M. Hebert: "Natural Terrain Classification Using Three-Dimensional Ladar Data for Ground Robot Mobility," *Journal of Field Robotics*, vol. 23, no. 10, pp. 839–861, 2006.
- [16] M. Bellone, A. Messina, and G. Reina: "A New Approach for Terrain Analysis in Mobile Robot Applications," *Proceedings of the 2013 IEEE International Conference on Mechatronics*, pp. 225–230, 2013.
- [17] H. Seraji: "Traversability Index: A New Concept for Planetary Rovers," *Proceedings of the 1999 IEEE International Conference on Robotics and Automation*, pp. 2006–2013, 1999.
- [18] A. Howard and H. Seraji: "Vision-Based Terrain Characterization and Traversability Assessment," *Journal of Field Robotics*, vol. 18, no. 10, pp. 577–587, 2001.
- [19] H. Seraji: "New Traversability Indices and Traversability Grid for Integrated Sensor/Map-Based Navigation," *Journal of Robotic Systems*, vol. 20, no. 3, pp. 121–134, 2003.
- [20] L. Huajun, Y. Jingyu, and Z. Chunxia: "A Generic Approach to Rugged Terrain Analysis Based on Fuzzy Inference," *Proceedings of International Conference on Control, Automation, Robotics and Vision*, pp. 1108–1113, 2004.
- [21] C. Ye and J. Borenstein: "A New Terrain Mapping Method for Mobile Robots Obstacle Negotiation," *Proceedings of the UGV Technology Conference at the 2003 SPIE AeroSense Symposium*, 2003.
- [22] Y. Lee, Y. Ji, J. Song, and S. Joo: "Performance Improvement of ICP-based Outdoor SLAM Using Terrain Classification," *Proceedings of the International Conference on Advanced Mechatronics 2010*, pp. 243–246, 2010.
- [23] E. H. Mamdani: "Application of Fuzzy Algorithms for Control of Simple Dynamic Plant," *Proceedings of the Institution of Electrical Engineers Control and Science*, vol. 121, no. 12, pp. 1585–1588, 1974.